

## Validating performance of automotive materials at high strain rate for improved crash design

P.K.C. Wood<sup>1</sup>, C. A. Schley<sup>1</sup>, S. Kenny<sup>1</sup>, T. Dutton<sup>2</sup>, M. Bloomfield<sup>3</sup>,  
R. Bardenheier<sup>4</sup>, J. R. D. Smith<sup>5</sup>

<sup>1</sup>University of Warwick, IARC\*, Central Campus, Coventry, CV4 7AL

<sup>2</sup>Dutton Simulation, 32 Lindsey Crescent, Kenilworth, Warwickshire, CV8 1FL

<sup>3</sup>Land Rover, Banbury Rd, Lighthorne, Warwick, CV35 0RG

<sup>4</sup>Instron Ltd, Coronation Rd, High Wycombe, Buckinghamshire, HP12 3SY

<sup>5</sup>ARRK Technical Services, Warwick Suite, Birmingham Rd, CV5 9QE

### Abstract

This paper investigates sources of performance variability in high velocity testing of automotive crash structures. Sources of variability, or so called *noise factors*, present in a testing environment, arise from uncertainty in structural properties, joint positions, boundary conditions and measurement system.

A box structure assembly, which is representative of a crash component, is designed and fabricated from a high strength Dual Phase sheet steel. Crush tests are conducted at low and high speed. Such tests intend to validate a component model and material strain rate sensitivity data determined from high speed tensile testing. To support experimental investigations, stochastic modelling is used to investigate the effect of noise factors on crash structure performance variability, and to identify suitable performance measures to validate a component model and material strain rate sensitivity data. The results of the project will enable the measurement of more reliable strain rate sensitivity data for improved crashworthiness predictions of automotive structures.

### Introduction

An improved understanding of the behaviour of automotive materials at high velocity is driven by the challenges of diverse crash legislation and competition amongst car manufacturers. The strength hardening effect of sheet steel under dynamic loading is widely reported in academic literature and is also recognized in the industry. New advanced high strength steels are seen to be increasingly attractive in those parts of the body-in-white with demanding performance requirements, leading to improved vehicle crashworthiness[1] and a potential for weight reduction. Design for performance must be matched with reliable material data as a basic input to simulation tools. This requirement is driven by the increasing sophistication of vehicle crash models in their numerical description. Uncertainty in the reliability of high speed tensile test data increases with strain rate and tensile data derived from strain rates as low as  $10\text{s}^{-1}$  exhibits appreciable variability[2]. The cost of generating high strain rate tensile data is also high and highly variable; using quasi-static test data as a datum, a small number of cost quotations received from a variety of academic and industry sources suggest a factor of 100 times higher in the extreme, but more generally costs fall between 40 to 60 times higher.

Strain rate sensitivity of sheet steel products must be accurately characterised in the performance range of interest to end users. This project aims to refine and standardize testing, characterization and validation processes, to enable the economic generation of reliable material strain rate sensitivity data for use in automotive crash simulation tools.

Investigations into existing full vehicle crash models and component based models within this project, suggest strain rates can reach on average  $60\text{s}^{-1}$  in a deforming crash structure. Local strain rates may reach  $500\text{s}^{-1}$  in component based models. Simulated strain measurements taken from the shell surface\* in the corner elements of component models can reach typically on average 30% effective strain and occasionally exceed 100%. This identifies the performance range required for generating reliable high speed tensile data; the strain range available in the tensile curve is from yield point to maximum stress.

### ***Variability in Quasi-static Material Tensile Data***

The figure 1 shows ten raw engineering stress strain curves derived from tension tests at low speed for a sheet steel product taken from the same coil, and tested in a common direction. The data appears smooth and continuous exhibiting low variability. For the material tested, yield point is measured at 0.2% proof offset and maximum tensile stress occurs at about 20% under quasi-static load. High accuracy and precision in deriving point properties in the range of interest *~ yield point to maximum tensile stress*, is expected from such smooth data.

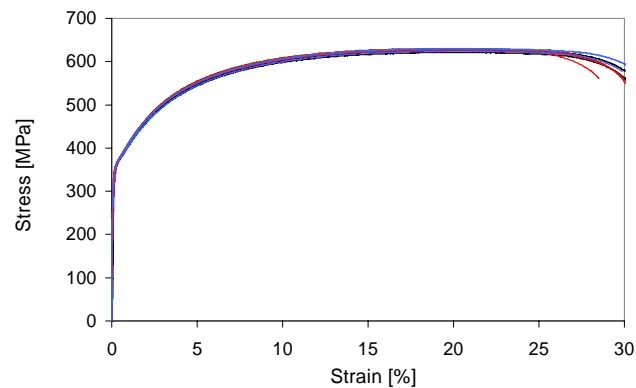


Figure 1. Engineering stress-strain data for DP600 steel tested in rolling direction under quasi-static loading (50mm gauge length / Euronorm test procedure[3]).

Such low performance variability could not be achieved in high velocity tensile testing due to the effects of various error sources. Sources of error in high velocity test data may be attributed to test machine type, inappropriate test controls, grip inertia, measurement system, specimen design and the interpretation of raw oscillatory test data.

## **Experimental Investigations**

### ***Experimental Equipment to Derive High Strain Rate Tensile Data***

A servo-hydraulic high speed test machine[4] has been procured to support this research project at the IARC. The test machine has an actuator velocity capable of delivering 20 m/s under open loop control, a Fast Jaw to grip specimen and data acquisition frequency of up to 5MHz. The machine control enables the Fast Jaw to grip specimen only once the actuator has reached target velocity.

The principle of operation requires the Fast Jaw grip to be accelerated in the direction of the white arrow in figure 2 to reach target velocity. On completion of the acceleration phase the knock out wedge is kicked out by a spacer rod pre-set by the test requirements, and the sprung grips released to grab the specimen in under  $5\ \mu\text{s}$  ( $5 \times 10^{-6}$  sec). Sensors in the machine system include Piezo load washer in the static grip head to measure force transmitted to test machine, linear variable differential transducer to measure actuator stroke position, and accelerometer mounted on the Fast Jaw. The signal from each sensor is recorded on a time base.

In addition to machine based sensors, strain gauges are placed on the specimen to measure a local response. One strain gauge placed at the centre of the gauge length and configured as a quarter bridge, measures plastic elongation to derive true strain and true strain rate. Strain gauges on the wider section of the fixed tab end, and configured as a full bridge to compensate for bending, measure an elastic elongation to derive true stress. The strain gauge is the best method for strain measurement at small strains especially when yield strength is of interest[5][6], but very high precision is normally restricted to 1% elongation, and typically adhesive or strain gauge failure occurs between 10% to 20%.

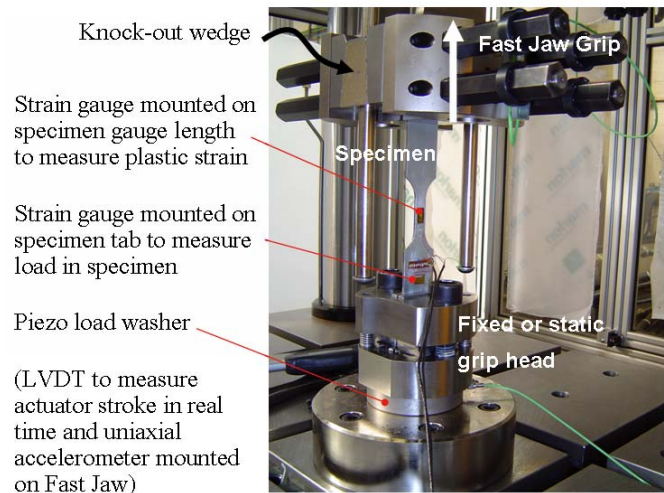


Figure 2. Tensile specimen assembled in high velocity servo-hydraulic test machine

These specimen-based sensors are especially important for measurements at high strain rate and may also be used to validate measurements derived from machine system based sensors.

**High Speed Tensile Specimen Design**

Specimen design for high speed tensile testing is a function of two dependencies - machine capability and desired strain rate. To a first approximation conventional strain rate is expressed by the formula grip velocity divided by initial gauge length and this is referred to as target strain rate. The high speed tensile specimen design shown in figure 3, will deliver a theoretical strain rate up to  $600s^{-1}$  with an actuator velocity of 15 m/s. The specimen gauge length is increased to 60mm and actuator speed reduced to 5 m/s to derive tensile data at lower strain rates  $< 80 s^{-1}$ .

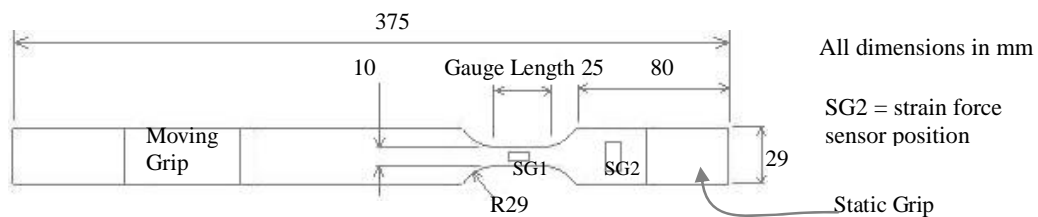


Figure 3. Specimen design for high velocity tensile test at 15 m/s

A Euronorm standard for high velocity testing is not in place, although recommendations for dynamic tensile testing of sheet steels has recently been published[5] [10] and this was used as a guide to the current high speed specimen design and development of test procedures.

**Calibration of Tensile Specimen Strain Gauges**

After placing strain gauges on the tensile specimen it requires calibration to obtain one force-voltage and one strain-voltage calibration curve, see figure 4. Therefore one additional specimen will be tested with a loadcell and clip gauge extensometer under quasi-static load to failure for this purpose.



Figure 4. Quasi-static calibration curves

### Raw High Velocity Tensile Test Data

Raw experimental data derived from high speed tensile testing at 5 m/s and 15 m/s is shown in figure 5 below. The initial gauge length of specimen in left figure is 60 mm and 25 mm in middle figure; target strain rates are respectively,  $80 \text{ s}^{-1}$  and  $600 \text{ s}^{-1}$ , although measured strain rate is typically 25% lower than target. The output from machine force sensor (piezo load washer) exhibits a low oscillating frequency estimated at 6kHz. At the higher speed of 15 m/s only three full oscillations develop from which to fit a curve, see middle figure; this is not robust. On the other hand, strain gauge force sensor mounted on specimen develops a higher oscillating frequency of 23kHz as shown in middle figure, and this enables a robust measurement of stress.

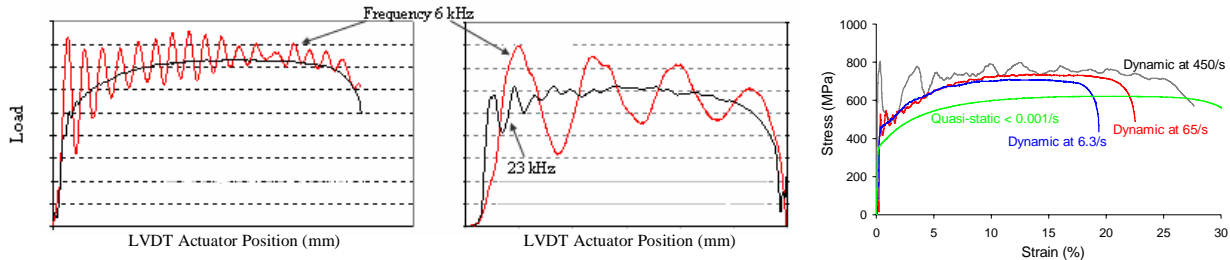


Figure 5. High speed test data generated at 5 m/s (left), 15 m/s (middle), set of raw engineering stress-strain strain rate dependent flow curves (right)

Raw tensile test data is processed to create a set of material flow curves with strain rate dependency; typically quasi-static ( $0.001 \text{ s}^{-1}$ ),  $5 \text{ s}^{-1}$ ,  $50 \text{ s}^{-1}$ ,  $500 \text{ s}^{-1}$  and formatted for use in a commercially available finite element code. Notice in figure 5 (right), the rate of strength hardening appears to diminish with increasing strain rate; this apparent non-linearity is widely reported in academic literature and recognized in the industry.

### Experimental Techniques to Validate High Strain Rate Tensile Data

A top hat box structure was selected in preference to other component geometries. This is because it was shown to deliver stable and consistent progressive lobe formation during crush following preliminary trials at low and high impact speed. The top hat assembly, shown in figure 6, consists of a fabricated open section (*top hat*) joined to a flat closure plate by spot welding. The box structure cross-section aspect ratio, spotweld positions along the flange together with initiator design, was determined using CRASHCAD software[7]. The initiator is introduced to box structure after assembly.

Equipment to conduct crush tests is a quasi-static electromechanical vertical test machine, and high speed impact sled test machine, both sited at Jaguar and Land Rover[8]. The test machines are fully instrumented together with test controls to deliver the required precision. The experimental set-up for quasi-static and impact crush tests is shown in the figure 7 below. The box structure is mounted on the moving sled for the impact test. A high speed camera is used to record the tests done on the sled test machine at 1000 fps. Three full lobes develop with each crushed specimen at high speed and similarly at quasi-static speed.

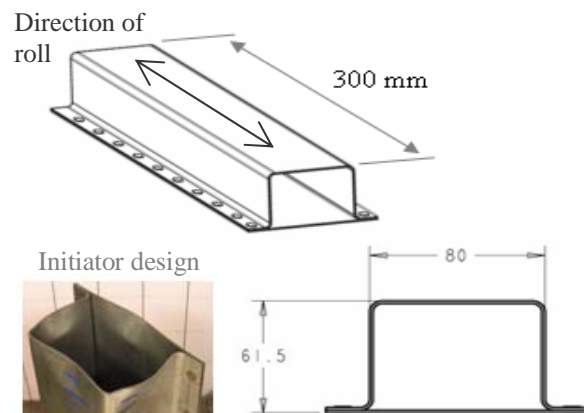


Figure 6. Top hat box structure joined by spot welding

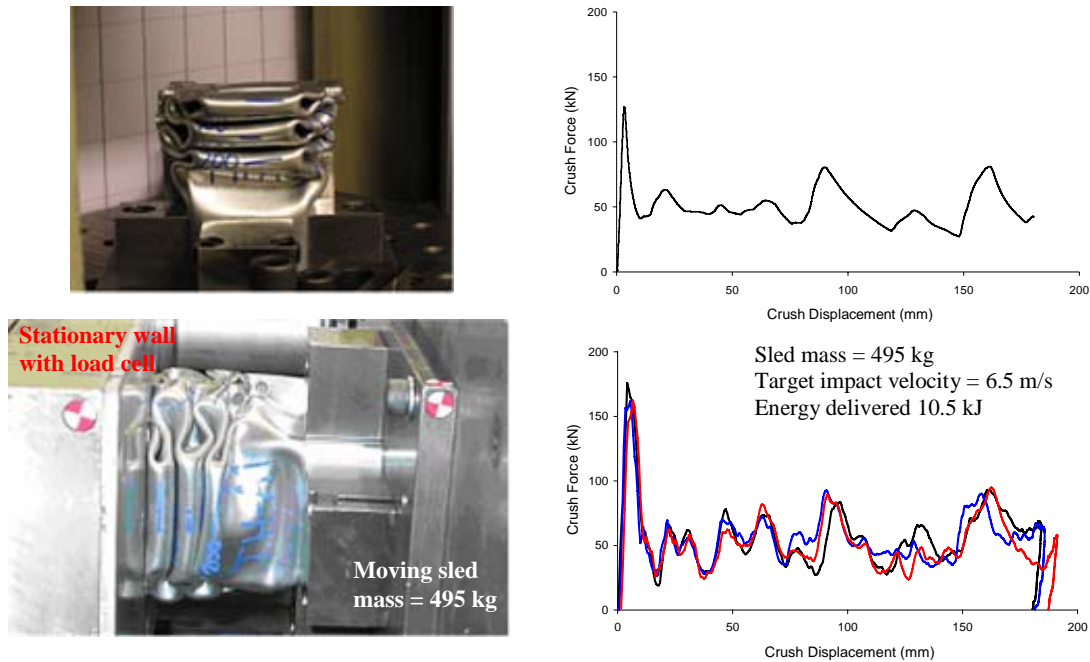


Figure 7. Experimental set-up: box structure crushed under quasi-static load on Zwick test machine (*upper left*), quasi-static crush result (*upper right*), box structure crushed under dynamic load on Sled test machine (*lower left*), three dynamic crush test results (*lower right*)

## Numerical Investigations

### *Modelling Variability*

The main sources of performance variability (*or so called noise factors*) in the sled impact test have been identified and measurements recorded where practical, see table 1 below. The measured range for each noise factor multiplied by an uncertainty factor is the input to a stochastic finite element model of the box structure. A finite element model of the experimental set-up is shown in figure 8. Model numerical properties conform to current best practice in the industry, noting the element size in the box structure is fixed at a 5mm square grid. The Monte Carlo method is used to generate 100 unique and independent model crush boxes for the noise factors considered. A two stage approach to validate component crush model and strain rate dependent material data has been considered.

### *Material Model*

In the first stage, which is the content of this paper, material strain rate dependency is not described by a full set of strain rate curves. Instead strain rate dependency is modelled using two curves. One curve is quasi-static stress-strain data the other curve is strain rate dependent stress-strain data measured at  $60\text{s}^{-1}$ . It is expected that the component crush model will deliver an over stiff response, resulting from the material model being stiffer at higher strain rate than suggested by the experimental tensile data, see also figure 5 (*right*).

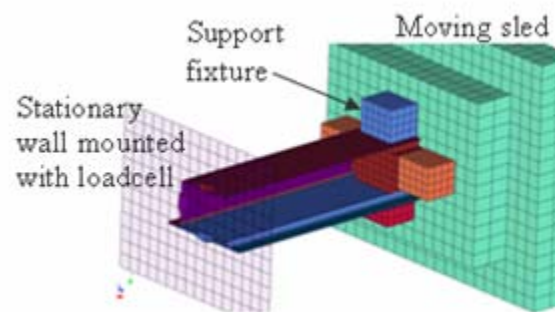


Figure 8. Model of experimental sled set-up

	Independent Noise Factor Variables	Nominal Input	Measured Range (+/-)	Uncertainty Factor	Distribution Model	Theoretical Coefficient of Variation *	No. of Runs
<b>Boundary Conditions</b>	Sled initial velocity	6.47 m/s (measured average)	+/- 0.1 m/s	2	Uniform	1.5%	100
	Stationary wall Align in Y plane	0 deg	+/- 1.5 deg	1	Uniform	Zero centred	100
	Stationary wall Align in Z plane	0 deg	+/- 1.5 deg	1	Uniform	Zero centred	100
<b>Material</b>	Top hat material yield stress offset	375 MPa	+/- 5 MPa	1	Uniform	1%	100
	Top hat material plastic flow curve scaling on stress-strain axes	Plastic multi-point data (120 data pts)	+/- 0.01	2	Uniform	5% (yield) 10% (UTS)	100
	Closure plate material yield stress offset	375 MPa	+/- 5 MPa	1	Uniform	1%	100
	Closure plate material plastic flow curve scaling on stress-strain axes	Plastic multi-point data (120 data pts)	+/- 0.01	2	Uniform	5% (yield) 10% (UTS)	100
<b>Geometry</b>	Gauge Top Hat	1.5 mm	+/- 0.02 mm	2	Uniform	1.5%	100
	Gauge Closure Plate	1.5 mm	+/- 0.02 mm	2	Uniform	1.5%	100
<b>Joints</b>	Spotweld 1 to n (Mat Spotweld) each randomly perturbed	Nominal defined in model geometry	+/- 2 mm	1	Uniform	n/a	100

(\*) 1/4 x measured range x uncertainty factor divided by nominal

Table 1. Noise factor variables in crush box and ranges applied in model

Variability in material data is measured from the quasi-static tensile test and a representative curve selected from the sample of ten curves shown in figure 1. Yield stress is derived using the 0.2% proof offset rule and describes a theoretical transition from elastic to plastic deformation. Plastic deformation is described using multi-point engineering stress-strain data. The simulation software is LS-DYNA[9] and material model type 24 is used to describe strain rate dependency.

The engineering quasi-static and strain rate curves are converted to true data and lightly filtered to create two smooth monotonically increasing flow curves originating from yield stress, see figure 9. The tensile flow curves are extended to 200% strain from maximum tensile stress using linear extrapolation. In this study random variation is introduced to strain rate dependent material model using a load curve format in LS-DYNA; and by offsetting stress on the stress axis, and scaling both stress and strain axes for the two flow curves shown in figure 9.

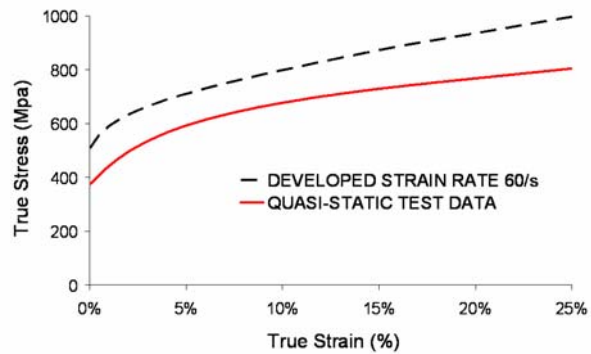
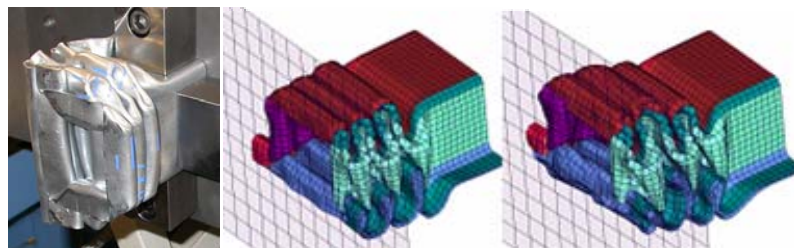


Figure 9. Material model with two strain rate load curve dependencies

### Results and Discussion

The figure 10 shows two of the one hundred sled test model crush structures in their final deformed state. The model crush deformation mode is consistent with the experiment.

Figure 10. Sled impact crush test (left), nominal model (middle), a random variable model (right)



Simulated raw data output from one hundred random variable input sled models is shown in figure 11. This will be used in data analysis.

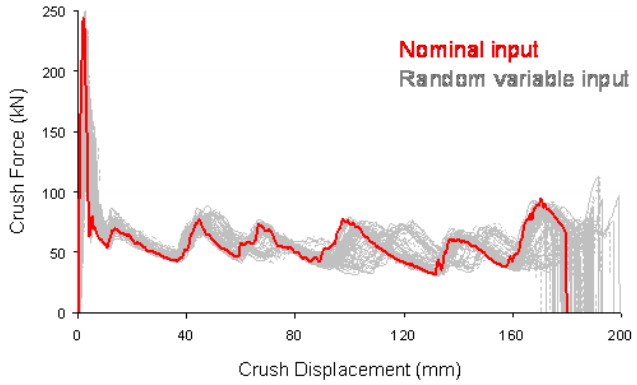


Figure 11. Force versus displacement data output from stochastic and nominal models

Frequency histograms for selected performance measures are shown in figure 12 below. None of the distributions suggest a good fit to a parent normal distribution model, and this is confirmed using a statistical goodness of fit test at 5% level of significance. In the left figure, maximum dynamic displacement exhibits two or more modes.

Total energy appears to follow a uniform parent distribution and average force (to maximum displacement) is slightly skewed to right. Notice nominal model is centred in the distributions except for average force. For convenience parametric statistics will be used in data analysis.

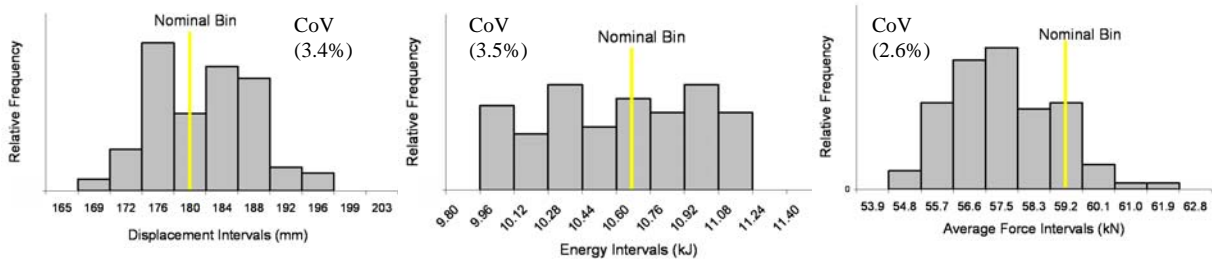


Figure 12. Distributions for maximum dynamic displacement (*left*), total energy (*middle*), average force (*right*)

Figure 13 is a bivariate plot of total energy versus average force. The quasi-static test result lies at some distance from both model and test data clusters, suggesting a measurable strain rate effect. An ellipse at two standard deviations is fitted to model and test sled data. A statistical test at 5% significance confirms no difference in the means (*ellipse centres*) between model and test sled data for total energy and average force. A difference in variability (*ellipse size*) observed between model and test sled data for total energy and average force is confirmed with a statistical test.

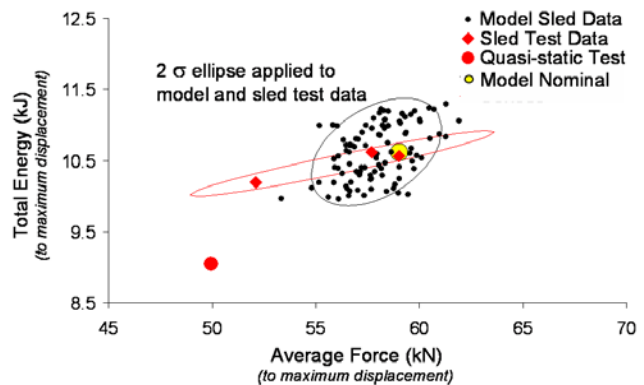


Figure 13. Bivariate plot of global performance measures total energy and average force

**Performance Dependency**

Performance variability is tuned by identifying model dependent inputs. The strength of a relationship between performance measures and noise factors may be measured by linear correlation ( $r$ ). High correlation offers a means to exert control. Consider first correlation between performance measures for the model sled data to identify couplings. Correlation between total energy and average force is ranked zero, see table 2 below; hence change to a dependent input for one will not accompany the other.

On the other hand, correlation between total energy and maximum displacement is ranked moderate; hence change to a dependent input for one will accompany a moderate change to the other. Therefore two of the three performance measures considered are sufficient to describe system performance.

Total energy has high dependency on boundary condition sled initial velocity (see table 2,  $r = +3$ ). Average force has moderate dependency on structural property top hat gauge ( $r = +2$ ). The effect of these two linearly dependent inputs on their respective performance measures is shown in figure 14 below. To validate model performance variability, a reduction in noise factor range for sled initial velocity to compress the model ellipse of figure 13 along the total energy axis is required; similarly an increase in top hat gauge will expand the model ellipse along the average force axis.

		Max Disp	Total Energy	Ave Force
Performance Measures	Maximum displacement		2	0
	Total energy	2		0
	Average force	0	0	
Boundary Conditions	Sled initial velocity	2	3	0
	Stationary wall Align in Y plane	0	0	0
	Stationary wall Align in Z plane	0	0	0
Structural Properties	Top hat material yield stress offset	0	0	0
	Closure plate material yield stress offset	0	0	0
	Top hat material plastic flow curve scaling on stress-strain axes	0	0	0
	Closure plate material plastic flow curve scaling on stress-strain axes	0	0	0
	Gauge top hat	-1	0	2
	Gauge closure plate	0	0	0

Table 2. Statistics based correlations between performance measures and noise factors using sled impact model data. Correlations between like performance measures are blanked.

Ranked by strength of correlation	
(3) High +/-	0.8 to 1.0
(2) Moderate +/-	0.6 to 0.8
(1) Weak +/-	0.4 to 0.6
(0) None	0 to 0.4

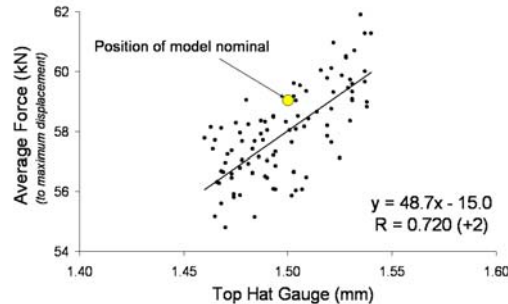
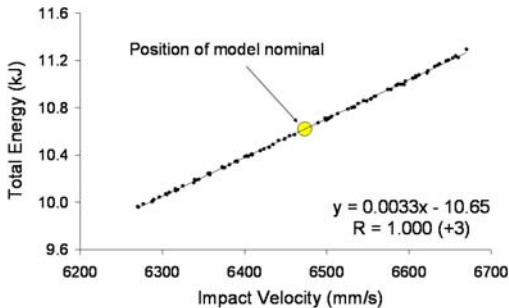


Figure 14. Effect of impact velocity on total energy (left), top hat gauge on average force (right)

The apparent linear dependency of sled impact velocity on total energy is surprising at first glance because energy is proportional to the square of velocity; because the noise factor range is comparatively low this non-linearity is not visible, but it is present. The uniform distribution obtained for total energy in figure 12 is a consequence of the high dependency on noise factor sled impact velocity, in which a uniform input distribution is used; hence a normal distribution is appropriate for this noise factor input. There is no statistical coupling between the material input on either total energy and average force performance measures.

**Search for Improved Performance Measures to Validate Sled Impact Model**

It was determined that there is no statistical difference between model and experimental sled impact means for total energy and average force to maximum displacement. In which case, a more complete set of metrics to validate sled impact model and material strain rate sensitivity must be established. Figure 15 plots average force computed over successive crush displacement intervals. Average force interval is computed as follows;

$$\text{Average Force Interval} = \frac{\text{Total Energy Absorbed in Crush Displacement Interval}}{\text{Crush Displacement Interval}}$$

For each crush displacement interval the derived energy and average force are now completely coupled, and either performance measure may be considered in analysis, but not both.



Comparing experimental sled impact and quasi-static results in figure 15, a difference in the average force means is observed for all crush displacement intervals; this is confirmed with a statistical test at 5% significance suggesting the presence of a strain rate effect. The largest difference in means occurs over the 0-20mm displacement interval and reaches an absolute difference of 33% [max-min/min]; the smallest absolute difference is 16% at 0-100mm.

Consider the model sled impact data in figure 15. Variability in average force interval (shown by error bar) is consistent across all crush displacement intervals, and is higher than that observed for the experimental sled impact data. Model nominal input is centred in all average force interval distributions with exception to crush displacement interval 0-20mm.

Model average force means are consistently higher than experimental sled impact means across all crush displacement intervals; the highest difference in means occurring at 0-60mm; because of the high performance variability in model data a statistical test at 5% significance confirms a difference in means for 0-20, 0-40, 0-60 and 0-80mm crush displacement intervals only; variability may be reduced by identifying dependent noise factors and reducing their respective range.

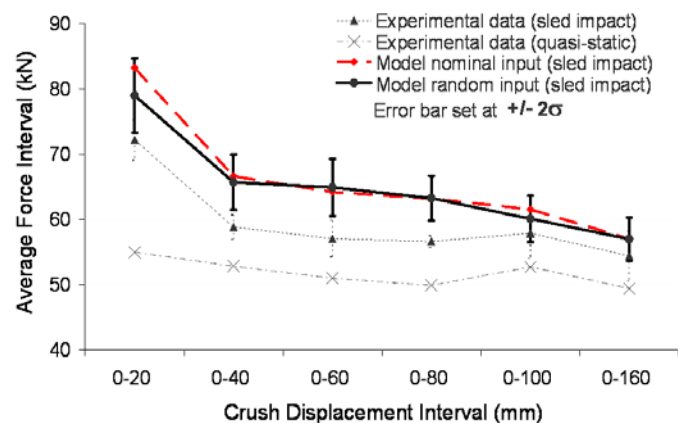


Figure 15. Average force over successive crush displacement intervals

Table 3 shows all average force intervals are moderately or highly correlated to structural property top hat gauge; for this performance measure there is no statistical dependency on any other input e.g. material, joints or boundary conditions, hence these are all excluded from the table. Further, correlation between average force to maximum displacement and all average force intervals is moderate to high, with exception to 0-60mm which is weak. Hence average force interval 0-60mm, is considered a necessary metric to validate sled impact model, and will have higher ranking than total energy and average force to maximum displacement because it shows the model to be over stiff in the means.

		Performance Measures							
		Total Energy (max disp)	Ave Force (max disp)	Ave Force Interval 0-20mm	Ave Force Interval 0-40mm	Ave Force Interval 0-60mm	Ave Force Interval 0-80mm	Ave Force Interval 0-100mm	Ave Force Interval 0-160mm
Performance Measures	Total Energy (to max disp)	0	0	0	0	0	0	0	0
	Ave Force (to max disp)	0	2	2	2	1	3	3	2
	Ave Force Interval 0-20mm	0	2	3	3	1	2	2	2
	Ave Force Interval 0-40mm	0	2	3	3	3	3	3	3
	Ave Force Interval 0-60mm	0	1	1	3	3	3	3	3
	Ave Force Interval 0-80mm	0	3	2	3	3	3	3	3
	Ave Force Interval 0-100mm	0	3	2	3	3	3	3	3
	Ave Force Interval 0-160mm	0	2	2	3	3	3	3	3
Boundary Conditions	Sled initial velocity	3	0	0	0	0	0	0	0
Structural Properties	Gauge top hat	0	2	2	3	2	3	3	3
		Ranked by strength of correlation							
		(3) High +/- 0.8 to 1.0							
		(2) Moderate +/- 0.6 to 0.8							
		(1) Weak +/- 0.4 to 0.6							
		(0) None 0 to 0.4							

Table 3. Statistics based correlations between performance measures and noise factors using sled impact model data. Correlations between like performance measures are blanked.

To validate sled impact model performance variability, a 50% reduction in noise factor range for velocity and gauge is proposed for the second stage analysis to follow; this may be implemented by reducing uncertainty factor to unity in both cases, see also table 1. A normal distribution will be applied to velocity noise factor.

The model sled impact data delivers a stiffer response than the experimental data which was anticipated, and is attributed to material strain rate sensitivity being represented by just one flow curve in addition to the quasi-static flow curve; the effect is to produce a considerably higher strength hardening effect for strain rates exceeding  $60\text{s}^{-1}$  that develop during dynamic deformation. To validate model performance mean, it is proposed in the analysis to follow, to describe material strain rate sensitivity using four flow curves; these are quasi-static,  $5\text{s}^{-1}$ ,  $50\text{s}^{-1}$  and  $500\text{s}^{-1}$ . This time quasi-static flow curve will retain a fixed input, and using the current nominal flow curve. A suitable noise factor range will be determined for the group of three strain rate dependent flow curves and implemented using yield offset and scaling functions.

### Concluding Summary

The experimental data suggests a measurable strain rate effect in the response of box structure under dynamic crush loading; the effect is consistent across all crush displacement intervals.

Performance measures to validate sled impact model and material strain rate sensitivity using a top hat box structure have been identified. As a minimum, total energy and average force to maximum displacement (maxima) together with average force for crush displacement interval 0-60mm are recommended, because there is a low coupling between these measures.

Comparing model and test sled impact data using maxima performance measures, there is no difference in the means; on the other hand using performance measure average force interval 0-60mm, model data exhibits higher variability and is considerably stiffer in the mean. The stiffer model response was expected and may be attributed to material strain rate sensitivity, in which strength hardening at higher strain rates has not been correctly modelled.

The model sled data has enabled noise factor inputs that have the strongest affect on performance variability to be identified. Boundary condition sled initial velocity affects total energy to maximum displacement, whilst structural property gauge affects average force for all crush displacement intervals to maximum displacement; hence performance measure average force is relatively isolated from the effects of test boundary conditions.

Model nominal input is generally centred in the model distributions for most performance measures and variability although higher than experimental data is still low (Coefficient of Variation < 5%). This suggests a deterministic approach may be used to validate model and material strain rate sensitivity data using the performance measures recommended.

### References

- [1] D. Cornette, T. Hourman, O. Hudin, J.P.Laurent, A. Reynaert, High Strength Steels for Automotive Safety Parts, SAE Technical Paper Series, 2001-01-0078.
- [2] [http://www.worldautosteel.org/pdf\\_hsrt/RptRndRobResults.pdf](http://www.worldautosteel.org/pdf_hsrt/RptRndRobResults.pdf)
- [3] BS EN 10002-1:2001 (low speed tensile testing of metallic materials and mechanical property characterisation).
- [4] VHS 160/100-20 High Strain Rate Test System and Accessories, Instron Ltd, Coronation Rd, High Wycombe, Bucks, England.
- [5] International Iron and Steel Institute (IISI) – High Strain Rate Experts Group, Recommendations for Dynamic Tensile Testing of Sheet Steels, pub August 2005.
- [6] K. Hoffmann, An Introduction to Measurements using Strain Gauges, pub 1989, Hottinger Baldwin Messtechnik GmbH, Darmstadt.
- [7] Impact Design Europe, CRASH CAD, UL. 3 Maja 18, Michalowice 05-816, Poland
- [8] Jaguar and Land Rover Vehicle Safety Test Laboratory, Banbury Rd, Lighthorne, Warwick, CV35 9RF, UK.
- [9] Ove Arup and Partners, Oasys LS-DYNA, The Arup Campus, Blythe Valley Park, Solihull, B90 8AE, UK.
- [10] STAHL-EISEN-Prüfblätter (SEP) des Stahlinstituts VDEh, The Determination of the Mechanical Properties of Sheet Metal at High Strain Rates in High-Speed Tensile Tests, SEP 1230, 1st Ed., April 2006.